New insight into the dispersion characteristics of electrostatic waves in ultradense plasmas: electron degeneracy and relativistic effects

Published in:
Plasma Physics and Controlled Fusion

Document Version:
Peer reviewed version

New insight in the dispersion characteristics of electrostatic waves in ultra-dense plasmas: electron degeneracy and relativistic effects

I. Kourakis[1], M. McKerr[1], I. S. Elkamash[1,2] and F. Haas[3]

[1] *Centre for Plasma Physics, Queen's University Belfast,*
BT7 1NN Northern Ireland, UK

[2] *Physics Department, Faculty of Science,*
Mansoura University, 35516 Mansoura, Egypt

[3] *Instituto de Física,*
Universidade Federal do Rio Grande do Sul,
Av. Bento Gonçalves 9500, Porto Alegre, RS, Brazil

The dispersion properties of electrostatic waves propagating in ultrahigh density plasma are investigated, from first principles, in a one-dimensional geometry. A self-consistent multispecies plasma fluid model is employed as starting point, incorporating electron degeneracy and relativistic effects. The inertia of all plasma components is retained, for rigor. Exact expressions are obtained for the oscillation frequency, and the phase and group velocity of electrostatic waves is computed. Two branches are obtained, namely an acoustic low-frequency dispersion branch and an upper (optic-like) branch: these may be interpreted as ion-acoustic and electron-plasma (Langmuir) waves, respectively, as in classical plasmas, yet bearing an explicit correction in account of relativistic and electron degeneracy effects. The electron-plasma frequency is shown to reduce significantly at high values of the density, due to the relativistic effect. The result is compared with approximate models, wherein either electrons are considered inertialess (low-frequency ionic scale) or ions are considered to be stationary (Langmuir-wave limit).

I. INTRODUCTION

The dynamics of dense plasmas in one-dimensional (1D) geometry is important, from a fundamental point of view, but also for practical applications [1]. Such systems are of relevance to the target normal sheath acceleration (TNSA) mechanism [2], during ultrahigh-intensity laser-matter interaction [3]. Applications range from dense quantum diodes [4] and electron-holes injected into quantum wires [5] to 1D fermionic Luttinger liquids [6]. Earlier studies have also focused on breather-modes in 1D semiconductor quantum wells [7] and Lagrangian structures in dense 1D plasmas [8].

The linear response of relativistically degenerate plasmas has been discussed, from first principles, in a number of earlier works. Tsytovich [9] discussed longitudinal and transverse wave propagation in a relativistic electron gas at high densities and temperatures, with particular attention to absorption due to pair production. Jancovici [10] discussed the dielectric properties of a high density relativistic electron gas at zero temperature in a positive background, using a quasi-boson formalism, which is equivalent to the random phase approximation. Hakim and Heyvaerts [11] extend the above descriptions by considering a covariant Wigner function formalism for a relativistic electron gas. (In the particular case of a fully degenerate equilibrium, the results of Ref. 10 are recovered.) We point out, to introduce our scope, here, that the above works have only focused on the electron gas dynamics (against a positive ion background), thus neglecting the ionic inertia and inevitably overlooking low-frequency ion-acoustic electrostatic waves. These have been included in later works [12, 13, 14, 15], where the ion component dynamics was properly taken into account.

From a fundamental point of view, the large value of the Fermi momentum in ultradense plasma configurations [13] may result in significant increase in the relativistic parameter p_F/mc [16], where p_F and m are respectively the Fermi momentum and the mass of the charge carriers, and c is the speed of light. Relativistic features and electron degeneracy effects may therefore operate hand in hand in such high density systems.

In this article, we investigate the dispersion characteristics of electrostatic waves in dense plasmas. To this end, we generalize a relativistic model for electrostatic excitations introduced recently [14, 17] by taking into account the inertia of both ion and electron component (fluids). Electron degeneracy is taken into account by an equation of state similar to Chandrasekhar's [18], albeit adapted to a 1D geometry [14, 19]. A cold (classical) ion fluid is considered, for simplicity.

Our work here focuses on plasma dynamics by adopting a one-dimensional (1D) geometry. In a broad context, 1D plasmas have been traditionally understood within the theory of 1D Coulomb systems, since the works by Lenard [20], Dawson [21] and Feix and co-workers [22, 23]. Originally, the adoption of an 1D geometry was justified to save effort and time in numerical computation. Recently, the exact analytical expression of the partition function in 1D colloidal systems has been obtained [24], following an earlier investigation of charge

screening in 1D Coulomb systems [25]. The comparison between quantitative prediction based on 1D theoretical considerations and their 3D counterpart inevitably involves certain ambiguities in interpretation, and requires a certain subtlety in manipulating dimensional analysis (and units). From a formal point of view, a correspondence between 1D and 3D plasmas is achieved by an assembly of parallel planes of charge. In this sense, the elementary charge becomes a surface density of charge, viz. $e = 1.6 \times 10^{-19} \, C/m^2$.

A relativistic multi-fluid plasma model is presented in the following Section II and its physical limitations are discussed. The dispersion properties of electrostatic waves are obtained and analyzed in Section III. A critical discussion of the relation to kinetic theory for electrostatic excitations is presented in Section IV. Simplified (approximate) versions for the dispersion relation are obtained in Section V, by considering various limits. The quantum-relativistic analogues of the ion-acoustic and electron plasma (Langmuir) mode(s) are obtained and analyzed in Sections VI and VII respectively. Finally, our results are discussed and summarized in the concluding Section VIII.

II. MULTIFLUID PLASMA MODEL

We consider an electron-ion plasma consisting of ions (mass m_i, charge $+e$) and relativistically-degenerate electrons (mass m_e, charge $-e$) A one-dimensional (1D) geometry is adopted for simplicity. In ultrahigh density conditions, electron degeneracy effects are significant: the electrons are thus assumed to obey a Fermi-Dirac distribution: a appropriate equation of state is employed for the electrons, providing the appropriate degeneracy pressure term in the highly relativistic limit. We assume from the outset that magnetic field generation may be neglected, within the electrostatic approximation, implying that the total current is zero (quiescent plasma).

Given their high mass, the ions will be treated as a cold (classical) fluid, for simplicity. The equations of motion for the ion fluid read:

$$\frac{\partial(\gamma_i n_i)}{\partial t} + \frac{\partial}{\partial x}(\gamma_i n_i v_i) = 0, \qquad (1)$$

$$\frac{\partial(\gamma_i v_i)}{\partial t} + v_i \frac{\partial(\gamma_i v_i)}{\partial x} = -\frac{e}{m_i} \frac{\partial \phi}{\partial x}, \qquad (2)$$

where e is the electron charge, m_i is the ion mass, n_i is the ion fluid density and v_i is the ion fluid speed. One distinguishes the electrostatic force $-e\partial\phi/\partial x = eE$ in the right-hand side (RHS), where E is the electric field deriving from an electrostatic potential function ϕ.

For the degenerate electrons, we shall adopt a fully relativistic fluid model proposed in Ref. 14. The electron

fluid equations read:

$$\frac{\partial(\gamma_e n_e)}{\partial t} + \frac{\partial}{\partial x}(\gamma_e n_e v_e) = 0, \qquad (3)$$

$$m_e H \left[\frac{\partial(\gamma_e v_e)}{\partial t} + v_e \frac{\partial(\gamma_e v_e)}{\partial x} \right] =$$

$$e\frac{\partial \phi}{\partial x} - \frac{\gamma_e}{n_e} \left(\frac{\partial P_e}{\partial x} + \frac{v_e}{c^2} \frac{\partial P_e}{\partial t} \right). \qquad (4)$$

In the latter expressions, H represents an enthalpy function $H = \sqrt{1 + \xi^2}$ [14], where the parameter $\xi = p_{Fe}/m_e c = h n_e/(4 m_e c)$ is related to the (high) electron density (note that ξ vanishes in the classical limit, $h \to 0$). In the latter expressions, m_e is the rest mass of the electron, n_e is the electron fluid (number) density and v_e is the velocity of the electron fluid, c is the speed of light *in vacuo*, h is Planck's constant.

The equations are obtained from the equations for an isotropic ideal fluid at rest by means of a Lorentz transformation [26]. One distinguishes the electrostatic term, in the RHS, along with a quantum relativistic pressure term emanating from the (1D) equation of state:

$$P_e = \frac{2m_e^2 c^3}{h} \left[\xi(1 + \xi^2)^{1/2} - \sinh^{-1} \xi \right]. \qquad (5)$$

This is essentially the the renowned Chandrasekhar equation of state [18], adapted to a 1D geometry [19] (for a critical discussion, see Ref. 14).

The relativistic factor $\gamma_{e,i} = 1/\sqrt{1 - v_{e,i}^2/c^2}$ appears in the fluid-dynamical equations, as a result of Lorentz transformations and relations among quantities (e.g. the electron and ion number density functions), between different inertial frames [14]. As also discussed earlier in Ref. 15, the fluid equations involve the proper densities and not the laboratory densities $N_{e,i} = \gamma_{e,i} n_{e,i}$. Certainly, one could formulate the basic equations in terms of $N_{e,i}$, but in this case, for the sake of coherence, one would be obliged to insert gamma factors inside the equations of state - a cumbersome option in our view.

The above (1D) equation of state for a degenerate relativistic electron gas, which is reminiscent of the Chandrasekhar (3D) equation of state used to describe equilibria in dense stars [18], was also derived by Chavanis in the context of white dwarf plasma equilibria [19]. The non-relativistic equation of state $P_e = p_F^2 n^3/(3 m_e n_0^2)$ is recovered for $\xi \ll 1$ (i.e., in the limit $c \to \infty$). Here, the subscript 0 denotes the value at equilibrium and $p_F = h n_0/4$ is the 1D expression of the Fermi momentum. The theory presented here therefore extends the earlier fluid theory for quantum ion-acoustic waves [27]. We have neglected quantum diffraction effects (via a Bohm potential term), since these are negligible in ultrahigh densities, compared to Fermi-Dirac statistical effects, except for ultra-small wavelengths [28]. The conditions of validity of the relativistic degenerate-electron cold-ion fluid model have been discussed, from first principle, in Ref. 14.

The system is closed by Poisson's equation:

$$\frac{\partial^2 \phi}{\partial x^2} = \frac{e}{\epsilon_0}(\gamma_e n_e - \gamma_i n_i)\,, \qquad (6)$$

where ϵ_0 denotes the permittivity of vacuum. Note that charge neutrality at equilibrium imposes $n_{e0} = n_{i0} = n_0$, where the subscript '0' indicates the equilibrium value (of the density, here).

III. LINEAR DISPERSION RELATION (EXACT)

We shall assume small harmonic variations around equilibrium, i.e. setting $n_{i,e} = n_0 + \tilde{n}_{i,e}\, e^{i(kx-\omega t)}$ (+ cc), $v_{i,e} = \tilde{v}_{i,e}\, e^{i(kx-\omega t)}$ (+ cc) and $\phi = \tilde{\phi}\, e^{i(kx-\omega t)}$ (+ cc), with the understanding that the tilded quantities are very small (compared to appropriate characteristic scales, e.g. $\tilde{n}_e \ll n_0$ and so forth) and that they are practically constant in space and time. (The usual acronym "cc" has been used to denote the complex conjugate.) One thus obtains a linear (Cramer) system for the amplitudes, in the form:

$$
\begin{aligned}
-\omega\, \tilde{n}_i + n_0 k\, \tilde{v}_i &= 0, \\
-m_i \omega\, \tilde{v}_i + ek\, \tilde{\phi} &= 0, \\
-\omega\, \tilde{n}_e + n_0 k\, \tilde{v}_e &= 0, \\
-m_e H_0\, \omega\, \tilde{v}_e + m_e \lambda k\, \tilde{n}_e - ek\, \tilde{\phi} &= 0, \\
-k^2 \tilde{\phi} + \frac{e}{\epsilon_0} \tilde{n}_i - \frac{e}{\epsilon_0} \tilde{n}_e &= 0
\end{aligned}
\qquad (7)
$$

where $H_0 = \sqrt{1+\xi_0^2}$, $\lambda = \frac{c^2 \xi_0^2}{n_0 \sqrt{1+\xi_0^2}}$ and $\xi_0 = \frac{hn_0}{4m_e c} = \frac{p_{F,0}}{mc}$ [14].

The condition for non-trivial solutions to exist is then expressed, after an algebraic manipulation, as

$$\omega^4 - \left[\omega_{p,e}^2 \left(\frac{1}{H_0} + \mu \right) + \frac{\xi_0^2}{1+\xi_0^2} c^2 k^2 \right] \omega^2 + \omega_{p,i}^2 \frac{c^2 k^2\, \xi_0^2}{1+\xi_0^2} = 0\,, \qquad (8)$$

where we have defined the mass ratio $\mu = m_e/m_i$ $(\ll 1)$ and the (ion or electron, respectively, for $j = i, e$) plasma frequency $\omega_{p,j} = \left(\frac{e^2 n_0}{\epsilon_0 m_j} \right)^{1/2}$. It is worth recalling that $\omega_{p,e}^2 \mu = \omega_{p,i}^2$. Solving this general relation, we obtain two branches: see Figs. 1 and 2. The lower curve (ω_-) corresponds to an acoustic mode (viz., $\omega_- = 0$ for $k = 0$). The upper curve (ω_+) corresponds to an optical-like mode, characterized by a frequency gap at $k = 0$:

$$\omega_+^2(k=0) = \omega_{p,e}^2 \left(\frac{1}{H_0} + \frac{m_e}{m_i} \right) = \omega_{p,e}^2 \left(\frac{1}{\sqrt{1+\xi_0^2}} + \frac{m_e}{m_i} \right)\,. \qquad (9)$$

This is essentially a modified Langmuir (electron plasma) mode. The cutoff frequency $\omega_0 = \omega_+(k=0)$ is
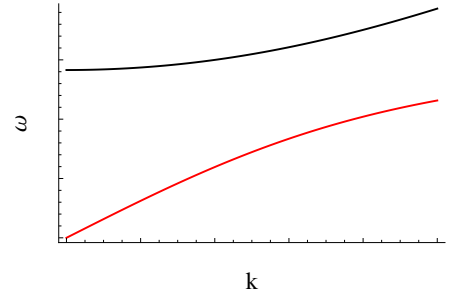

FIG. 1: A heuristic plot (off scale) of the dispersion relation (8). The lower curve (red) is an ion-acoustic mode, while the upper (black) curve, featuring a finite cutoff frequency, represents a quantum-relativistic electron plasma (Langmuir) mode.

slightly higher than the electron plasma frequency $\omega_{p,e}$ in the classical limit, viz. $\omega_0 \to \omega_{p,e}[1 + m_e/(2m_i)] \approx 1.00025\,\omega_{p,e}$ in the "classical" limit $\xi_0 \to 0$, due to the finite electron inertia being retained (see that the latter expression would reduce to $\omega_0 \simeq \omega_{p,e}$, should one neglect the electron inertia, as expected, since $m_e \ll m_i$). Furthermore, in the weakly relativistic case $\xi_0 \ll 1$, $\omega_0 \simeq \omega_{p,e}[1 - \xi_0^2/4 + m_e/(2m_i)]$. However, at high densities, viz. $\xi_0 \gg 1$, the cutoff frequency (representing essentially non-propagating electrons oscillations) reduces dramatically, due to the relativistic effect: see that $\omega_0 \sim \omega_{p,e}/\xi_0^{1/2}$ for $\xi_0 \gg 1$. The cutoff frequency expressed in (9) may take the alternative form

$$\omega_+^2(k=0) = \omega_{p,i}^2 + \omega_{p,e}^2 / \sqrt{1+\xi_0^2}\,, \qquad (10)$$

reflecting the fact that the electron-plasma oscillation eigenfrequency is modified due to quantum-relativistic corrections, but also due to the finite ionic inertia having been retained.

The latter relations may be simplified further, recalling the definition $\xi_0 = hn_0/(4m_e c)$, viz. substituting with $\xi_0^2 c^2 = h^2 n_0^2/(4m_e)^2$ where appropriate. It is straightforward to see that the wavenumber k enters the dispersion relation only via the function, say Ω_k^2, defined by:

$$\Omega_k^2 = \frac{c^2 k^2\, \xi_0^2}{1+\xi_0^2} = \frac{\left(\frac{hn_0}{4m_e}\right)^2 k^2}{1 + \left(\frac{hn_0}{4m_e c^2}\right)^2} = \frac{c_0^2 k^2}{1 + \left(\frac{c_0^2}{c^2}\right)^2}\,. \qquad (11)$$

It was simply a matter of physical intuition to define the quantity $c_0 = \frac{hn_0}{4m_e}$ $\left(= \frac{p_{F,e}}{m_e}\right)$ [14] as a characteristic speed, essentially representing here the equivalent of an acoustic (sound) speed, in the quantum-relativistic model.

The above two branches are shown in Fig. 2. We see that both frequencies (acoustic and Langmuir-like branch) increase, for higher density values.

It is worth pointing out that, for ease of algebraic manipulation, one may cast the dispersion relation in the form:

$$\omega^4 - \left(\tilde{\omega}_{p,e}^2 + \omega_{p,i}^2 + \Omega_k^2 \right) \omega^2 + \omega_{p,i}^2\, \Omega_k^2 = 0\,, \qquad (12)$$
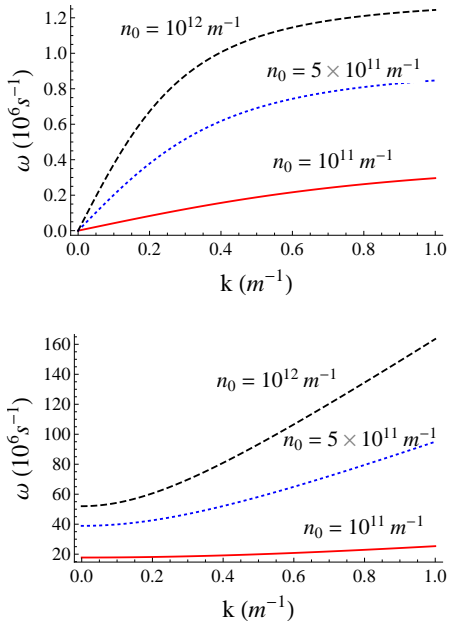
FIG. 2: The acoustic "lower" mode (top panel) and the Langmuir- (optical-)like "upper" mode (bottom panel) are depicted, as derived numerically from relation (8). The angular frequency ω is shown versus the wavenumber k for different values of the equilibrium density n_0. Top to bottom, the values of ξ_0 are: $\xi_0 \approx 0.6, 0.3, 0.06$, respectively, for $n_0 = 10^{12}, 5 \times 10^{11}, 10^{11} m^{-1}$.

where all quantities were defined above except $\tilde{\omega}_{p,e}^2 = \omega_{p,e}^2/H_0 = \omega_{p,e}^2/\sqrt{1+\xi_0^2}$.

IV. COMPARISON WITH KINETIC THEORY

To validate our results presented above, based on the fluid model, it would be interesting to compare with the results from the 1D relativistic Vlasov-Poisson system, which reads

$$\frac{\partial f_e}{\partial t} + \frac{p}{\Gamma_e m_e}\frac{\partial f_e}{\partial x} - eE\frac{\partial f_e}{\partial p} = 0 \,, \quad (13)$$

$$\frac{\partial f_i}{\partial t} + \frac{p}{\Gamma_i m_i}\frac{\partial f_i}{\partial x} + eE\frac{\partial f_i}{\partial p} = 0 \,, \quad (14)$$

$$\frac{\partial E}{\partial x} = \frac{e}{\varepsilon_0}\Big(\int_{-\infty}^{\infty} f_i dp - \int_{-\infty}^{\infty} f_e dp\Big), \quad (15)$$

where $f_{e,i} = f_{e,i}(x,p,t)$ denote the phase space electron and ion probability distribution functions and $\Gamma_{e,i} = \sqrt{1 + p^2/(m_{e,i}^2 c^2)}$. As above, we neglect ion temperature effects, so that the equilibrium ion distribution function will be $f_i^0 = n_0\delta(p)$. Denoting $f_e^0 = f_e^0(p)$ as the equilibrium electron distribution function and linearizing by following the usual procedure [15, 29], one derives the

relativistic dispersion relation

$$1 = \frac{\omega_{pi}^2}{\omega^2} + \frac{\omega_{pe}^2}{n_0}\int_{-\infty}^{\infty} \frac{dp f_e^0(p)}{\Gamma_e^3\left(\omega - \frac{kp}{m_e\Gamma_e}\right)^2} \,. \quad (16)$$

We are especially concerned with the real part of the kinetic dispersion relation, so that the principal value (denoted as f) is understood in the integral in Eq. (16).

Considering the 1D degenerate normalized electronic equilibrium: $f_e^0 = n_0/(2p_{Fe})$ for $|p| < p_{Fe}$; $f_e^0 = 0$ for $|p| > p_{Fe}$, we find

$$1 = \frac{\omega_{pi}^2}{\omega^2} + \frac{\omega_{pe}^2\sqrt{1+\xi_0^2}}{(1+\xi_0^2)\,\omega^2 - \xi_0^2 c^2 k^2} \,, \quad (17)$$

which is exactly the same as the fluid dispersion relation, namely

$$1 = \frac{\omega_{pi}^2}{\omega^2} + \frac{\omega_{pe}^2}{\sqrt{1+\xi_0^2}\,\omega^2 - (k^2/m_e)(dP_e/dn_e)_0} \quad (18)$$

also shown in Eq. (8), as can be verified using the 1D equation of state (5). It should be noted that the full agreement observed here between the fluid dispersion relation and the (real part of) the kinetic dispersion relation is a special feature of the 1D geometry.

V. APPROXIMATE EXPRESSIONS

A. Small frequency limit

Assuming $\omega \ll \left(\tilde{\omega}_{p,e}^2 + \omega_{p,i}^2 + \Omega_k^2\right)^{1/2}$ (see definitions above), the quartic term ω^4 may be neglected. The dispersion relation then simplifies to:

$$\begin{aligned}\omega_{-,approx}^2 &\approx \frac{\omega_{p,i}^2\,\Omega_k^2}{\tilde{\omega}_{p,e}^2 + \omega_{p,i}^2 + \Omega_k^2} \\ &= \omega_{p,i}^2\frac{c_0^2 k^2}{1+\left(\frac{c_0^2}{c^2}\right)^2}\frac{1}{\tilde{\omega}_{p,e}^2 + \omega_{p,i}^2 + \frac{c_0^2 k^2}{1+\left(\frac{c_0^2}{c^2}\right)^2}}\,. \quad (19)\end{aligned}$$

This is essentially the analogue of the ion-acoustic mode in the quantum-relativistic model, where the thermal pressure of the electrons (reflected in the classical textbook [30] definition of the sound speed, $c_s = (k_B T_e/m_i)^{1/2}$, which is related to the electron temperature T_e; k_B being the Boltzmann constant) is here substituted by the Fermi-energy related pressure (manifested in the above expression for the characteristic speed $c_0 = (E_{F,e}/m_i)^{1/2}$).

B. High frequency limit

It can be verified that, for all density values high enough to be of relevance in our model, the coefficient of

the quadratic term in the bi-quadratic polynomial equation (12) above (and in all of its preceding alternative forms) exceeds the constant term by far. It can thus be

shown that the upper (Langmuir-type) frequency mode is approximately given by:

$$\omega_{+,approx}^2 \approx \frac{\omega_{\mathrm{pe}}^2}{\sqrt{1+\xi_0^2}} + \omega_{\mathrm{pi}}^2 + c^2 k^2 \xi_0^2 \left[\frac{1}{1+\xi_0^2} - \frac{\omega_{\mathrm{pi}}^2}{\xi_0^2 \left(c^2 k^2 + \omega_{\mathrm{pi}}^2 \right) + \sqrt{1+\xi_0^2}\, \omega_{\mathrm{pe}}^2 + \omega_{\mathrm{pi}}^2} \right]. \tag{20}$$

For small values of the wavenumber k, this expression can be approximated as:

$$\omega_{+,approx}^2 \approx \frac{\omega_{\mathrm{pe}}^2}{\sqrt{1+\xi_0^2}} + \omega_{\mathrm{pi}}^2 + \frac{\xi_0^2}{1+\xi_0^2}\, \frac{\omega_{\mathrm{pe}}^2 c^2 k^2}{\omega_{\mathrm{pe}}^2 + \sqrt{1+\xi_0^2}\, \omega_{\mathrm{pi}}^2}$$
$$\equiv \omega_0^2 + C_0^2 k^2. \tag{21}$$

This is visibly a parabolic function in the wavenumber k, which is analogous to the known textbook functional form for (classical) Langmuir waves, viz. $\omega^2 = \omega_{p,e}^2 + c_{th,e}^2 k^2$, where $c_{th,e} = (k_B T_e/m_e)$ [30], where both frequency cutoff and characteristic speed are hereby modified due to quantum relativistic corrections, incorporated in our model.

Note that the frequency cutoff ω_0 satisfies Eq. (10) above, as expected. Furthermore, the characteristic speed C_0:

$$C_0 = \left(\frac{\xi_0^2}{1+\xi_0^2} \right)^{1/2} \left(\frac{\omega_{\mathrm{pe}}^2}{\omega_{\mathrm{pe}}^2 + \sqrt{1+\xi_0^2}\, \omega_{\mathrm{pi}}^2} \right)^{1/2} c$$
$$= \left(\frac{\xi_0^2}{1+\xi_0^2} \right)^{1/2} \left(\frac{1}{1+\frac{m_e}{m_i}\sqrt{1+\xi_0^2}} \right)^{1/2} c \tag{22}$$

behaves as

$$C_0 \approx \left(\frac{1}{1+\frac{m_e}{m_i}} \right)^{1/2} \xi_0\, c \simeq \frac{hn_0}{4m_e} = \frac{p_{F,0}}{m_e},$$

in the small density ($\xi_0 \ll 1$) limit. This expression coincides with the pseudo-"sound" speed defined above. On the other hand, for large values of the density (viz. $1 \ll \xi_0 \ll m_i/m_e$), the characteristic speed C_0 approaches c, as inferred from (22).

It should be noted here, for rigor, that our electrostatic model breaks down for ultrahigh-densities, where quantum electrodynamic effects (neglected here) are dominant.

VI. QUANTUM-RELATIVISTIC ION-ACOUSTIC WAVES

The conventional method to describe ion-acoustic waves is by neglecting the electron inertia from the outset. In the classical picture, one considers an ion

fluid, surrounded by an electron cloud which, given the large mass disparity between electrons and ions, can be considered to be at thermal equilibrium, viz. $n_e = n_{e,0} \exp(e\phi/(k_B T_e))$. The classical, non-relativistic dispersion relation thus obtained reads

$$\omega^2 = \omega_{p,i}^2 \frac{k^2}{k^2 + k_D^2}, \tag{23}$$

where $k_D^2 = e^2 n_0/(\epsilon_0 k_B T_e)$ in the inverse Debye length (square) [30].

In our case, this physical situation can be reproduced by neglecting the electron inertia, i.e. by ignoring the convective term in the left-hand of the momentum equation (4), for the electron fluid. It is a matter of straightforward algebra [31] to obtain the "ion-acoustic" wave dispersion relation:

$$\omega_{IA}^2 = \omega_{p,i}^2 \frac{k^2}{k^2 + \lambda_{scr}^{-2}}, \tag{24}$$

where we have defined the charge screening length as $\lambda_{scr} = \left(\frac{2\epsilon_0 E_{Fe,0}}{n_0 e^2} \right)^{1/2} \sqrt{1+\xi_0^2} = \left(\frac{\epsilon_0 m_e c^2 \xi_0^2}{n_0 e^2} \right)^{1/2} \sqrt{1+\xi_0^2} = \left(\frac{\epsilon_0 h^2 n_0}{16 m_e e^2} \right)^{1/2} \sqrt{1 + \left(\frac{hn_0}{4m_e c} \right)^2}$ (the classical, i.e. non-relativistic definition of the Fermi energy $E_{Fe} = p_{Fe}^2/2m_e$ was adopted here). The last relation for the ion-acoustic frequency coincides with the one derived in Ref. 32.

It may be appropriate to compare the ion-acoustic dispersion relation (24) to the approximate relation (19) obtained earlier. The two expressions are close for small equilibrium density, but begin to diverge as a higher density results in a larger relativistic electron mass, as expressed via the factor $m_e \sqrt{1+\xi_0^2}$. This relativistic mass may not, properly speaking, compare to the ion mass for reasonable densities ($n_0 \lesssim 10^{12} m^{-1}$ in 1D), but it certainly entails a definite variation: see Fig. 3.

We have derived three versions of the low-frequency (ion-acoustic) mode, namely: (i) the lower root ω_- of the exact relation (8), deriving from the two-fluid model, (ii) the approximate form $\omega_{-,approx}$ given by (19), and (iii) ω_{IA}, given by (24), which was derived from the ion-fluid model (neglecting electronic inertia). These three curves are shown in Fig. 3, for an indicative density

value $n_0 = 10^{11} m^{-1}$ (roughly equal to the cubic root of a density characteristics of the interior of a white dwarf star [33]). We see that the exact dispersion relation and its approximation are almost identical, while ω_{IA} lies just above the other two: taking electron inertia into account therefore slightly increases the ion-acoustic frequency.
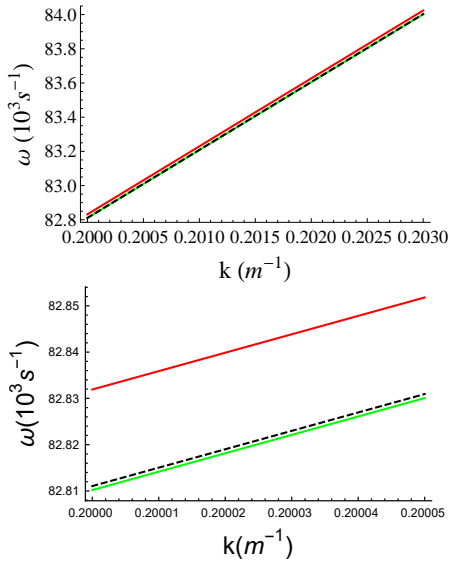

FIG. 3: (Top panel) The low-frequency (ion acoustic) mode is depicted, as obtained from three different functional relations: the exact (two-fluid) dispersion relation (8) (black, dashed), the approximation (19) to this (green) and the dispersion relation (24) derived from the ion-fluid model (i.e. neglecting the electron inertia). The angular frequency ω is shown versus the wavenumber k. We have taken $n_0 = 10^{11} m^{-1}$ for the plot (i.e., a value roughly equal to the cubic root of a density characteristic of the interior of a white dwarf star [33]). (Bottom panel) As above: closeup view near the origin.

VII. QUANTUM-RELATIVISTIC ELECTRON PLASMA (LANGMUIR) WAVES

Let us now consider a different physical limit. Suppose that the ions are so slow, relative to the electrons, as to be effectively static. It is then safe to neglect the ion-fluid equations (1, 2), assuming that $n_i =$constant. It is straightforward, upon linearization, to find the electron plasma dispersion relation:

$$\omega_{EP}^2 = \frac{e^2 n_0}{\epsilon_0 m_e \sqrt{1+\xi_0^2}} + \frac{\xi_0^2}{1+\xi_0^2} c^2 k^2$$
$$\equiv \omega_{p,e}^2 / \sqrt{1+\xi_0^2} + V_0^2 k^2. \qquad (25)$$

One easily recognizes in the first term in the RHS the expression recovered from the relativistic Langmuir frequency (9) or (10) above, upon setting the ion mass to infinity. Furthermore, the characteristic speed $V_0 = \left(\frac{\xi_0^2}{1+\xi_0^2}\right)^{1/2} c = \left[\frac{(hn_0/4m_ec)^2}{1+(hn_0/4m_ec)^2}\right]^{1/2} c = \left[\frac{c_0^2}{1+(hn_0/4m_ec)^2}\right]^{1/2}$

defined above is related to the Fermi speed (the characteristic speed c_0 was defined above). It is straightforward to show that (25) above is exactly recovered from the exact 2-fluid dispersion relation (12) above – recalling definition (11) – upon setting $\omega_{p,i}$ to zero (i.e., in the infinite ion mass limit), as intuitively expected. This mirrors the structure of the classical, non-relativistic equivalent:

$$\omega^2 = \omega_{p,e}^2 + 3v_{th}^2 k^2 , \qquad (26)$$

upon formally substituting the thermal velocity with V_0.

It appears imposed to compare the latter dispersion relation with the approximate solution (21) of the exact dispersion relation (8): In fact, (21) approaches (25) as one cancels the ion plasma frequency or, alternatively, as the equilibrium density increases, since the static ion assumption gains validity as electron Fermi energy increases.

Summarizing our findings for the high-frequency (Langmuir-like) mode, we have derived three versions of the dispersion relation, namely: (i) the upper branch ω_+ of the exact relation (8), deriving from the two-fluid model, (ii) the approximate form $\omega_{+,approx}$ given by (21), and (iii) ω_{EP}, given by (25), which was derived from the electron-fluid model (considering an infinite ion inertia). These three curves are shown in Fig. 4 (for an indicative density value $n_0 = 10^{11} m^{-1}$, roughly equal to the cubic root of a density characteristic of the interior of a white dwarf star [33]. We see that the exact dispersion relation and its approximation are almost identical, while ω_{EP} lies below the other two: taking finite ion inertia into account therefore slightly increases the electron-plasma frequency.

.

VIII. DISCUSSION

We have derived the new dispersion relation (8) for ultradense (quantum) plasmas modelled by introducing a relativistic multi-fluid model, taking into account the finite inertia of both electron and ion fluids. In other words, no simplifying hypothesis was adopted, e.g. of a vanishing electron inertia (for ionic excitations) or, reversely, of infinite inertia (stationary state) for ions (as regards high-frequency electron plasma waves). This new dispersion relation, bearing the form of a quartic polynomial, reduces to the approximate dispersion relations (24) and (25), which agree with expressions earlier derived for ion-acoustic and electron plasma waves, respectively [14, 17]. This agreement was confirmed numerically for both low- and high-frequency branches. This agreement is also reflected in the phase speed and group velocity, as shown in Figures 5 and 6. In the former (Fig. 5), the exact relation (8), and the approximations (19) and (24) are seen to be practically indistinguishable. In a similar manner, in Fig. 6, the exact relation (8), and the approximations (20) and (25) also overlap almost perfectly. Recall that for a modulated envelope wave, the
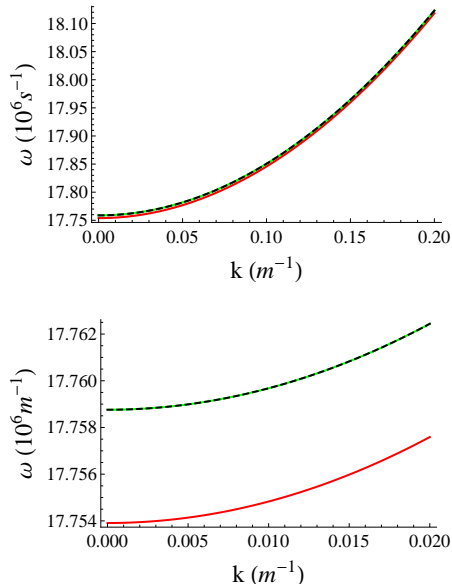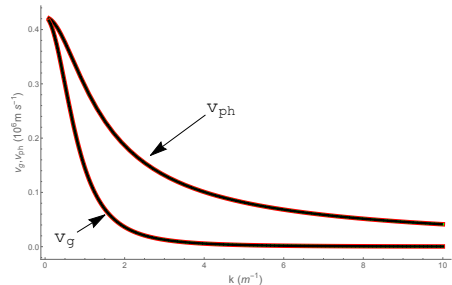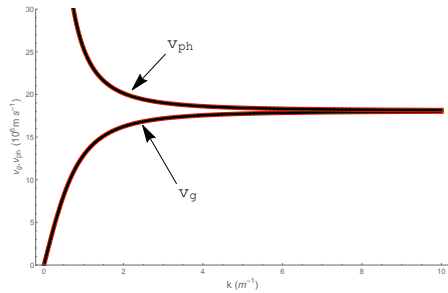
FIG. 6: The phase speed $v_{ph} = \omega/k$ and group velocity $v_g = d\omega/dk$ for the Langmuir dispersion curve. Note that both curves tend to a constant asymtotic value for large wavenumber (short wavelength) values.

phase speed values differ substantially between successive values of the density, and in fact increase for higher density value (this is true for both dispersion modes, i.e. in both of the latter figures).

FIG. 4: Top panel: The electron plasma (Langmuir) mode is plotted here, as obtained from three different functional relations: the exact (two-fluid) dispersion relation (8) (black, dashed), the approximation (20) to this (green) and the dispersion relation (25) (red, bottom curve) derived from the electron-fluid model (i.e. for an infinite ion inertia). Bottom panel: closeup view for small k. We have taken $n_0 = 10^{11} m^{-1}$ for the plots, as in Fig. 3.

carrier waves move at phase speed while the wave envelope moves at the group speed.

FIG. 5: The phase speed $v_{ph} = \omega/k$ and the group velocity $v_g = d\omega/dk$, for the ion-acoustic dispersion curve. Note that both curves tend to zero for large wavenumber (short wavelength) values.
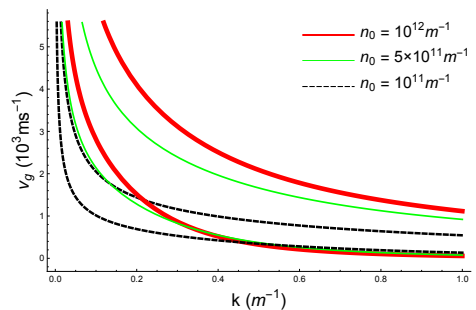
FIG. 7: The group velocity v_g and the phase speed v_{ph} of the low-frequency (ion-acoustic) dispersion mode is shown, for different values of the electron number density. The thick (red), thin (green) and dashed (black) curves are as described in the inset label. For each pair of same colour/style, the top curve corresponds to the phase speed, while the bottom one to the group velocity).

It was shown earlier that the relativistically-degenerate system only begins to distinguish itself from the non-relativistic version at high density values ($n_0 \gtrsim 10^{11} m^{-1}$); recall the dependence of the dispersion characteristics on the density n_0 via the variable ξ_0; also, note Fig. 2. To investigate the dependence of the propagation characteristics on the electron (number) density, we have depicted the group- and phase speed of the lower (ion-acoustic) and upper (optical-like, electron plasma) modes, for various values of the number density, in Figures 7 and 8, respectively. We see that both group- and
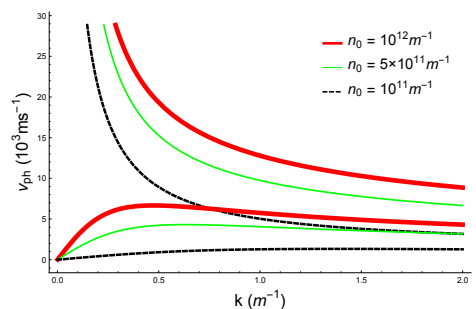

FIG. 8: The group velocity v_g and the phase speed v_{ph} of the high-frequency (electron plasma) dispersion mode is shown, for different values of the electron number density. The thick (red), thin (green) and dashed (black) curves are as described in the inset label. For each pair of same colour/style, the top curve corresponds to the phase speed, while the bottom one to the group velocity).

The density dependence discussed above is intuitively expected, if one recalls the expression for the Fermi energy: $E_{Fe} = m_e c^2 \left(\sqrt{1 + p_F^2/m_e^2 c^2} - 1 \right)$, to be compared to the non-relativistic working expression $E_{Fe} = p_F^2/2m_e$. A comparison of the resulting numerical value of the Fermi energy, which also influences the "Debye" screening length $\lambda_D = \sqrt{\frac{2\epsilon_0 E_{Fe}}{e^2 n_0}}$, is given in Fig. 9. We see that deviation from the non-relativistic regime requires high density values. For low densities, in other words, the non-relativistic formulation is sufficient.
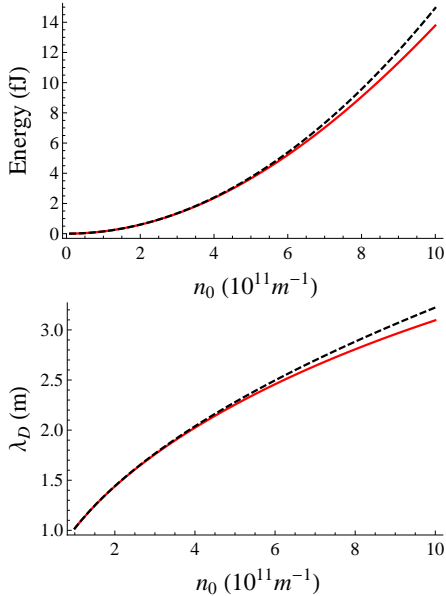
FIG. 9: The Fermi energy (top panel) and the "Debye" screening length (bottom panel) for relativistically-degenerate (red, continuous line) vs. degenerate, but non-relativistic (black, dashed line) plasma systems is depicted.

The relativistically-degenerate theory is valid under certain assumptions. The temperature and density must be of such a magnitude that the relativistic Fermi energy exceeds both the non-relativistic Fermi energy and the thermal energy. Figures 10 and 11 show how the exact dispersion relation (8) compares with the classical, non-relativistic equivalent under conditions which might be found in the interior of a white dwarf ($n_{1D} = 10^{11} m^{-1}$, $T = 10^5 K$). In the above plots, the relativistic quantum relations approach the non-relativistic classical equivalents as the density is reduced (for a given temperature). Using a simple, heuristic argument, one may approximate the density value for which the two descriptions are approximately equal by depicting the boundary line ($E_{Fe} = k_B T_e$) – see Fig. 12 – which delimits the range of temperatures and densities for which the quantum framework is valid (i.e., in the grey area in this plot).

It may be noted that, according to the general theory of 1D Coulomb systems [22], the "graininess" parameter in our case is defined as $g = 1/(n_0 \lambda_D)$, which is much smaller than unity as can be seen from Figure
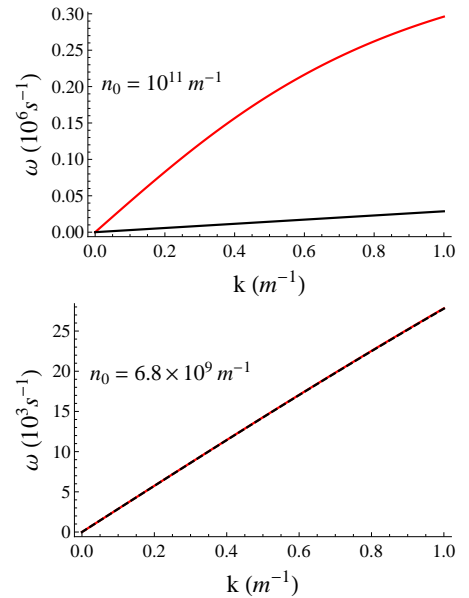

FIG. 10: A comparison between the relativistic and classical ion-acoustic dispersion curve(s): the exact relation (8) in red and the classical non-relativistic in black. We have taken $T = 10^5 K$ in both cases. Note that $\xi \approx 0.06$ in the upper panel, while $\xi_0 = 0.004$ in the lower panel.
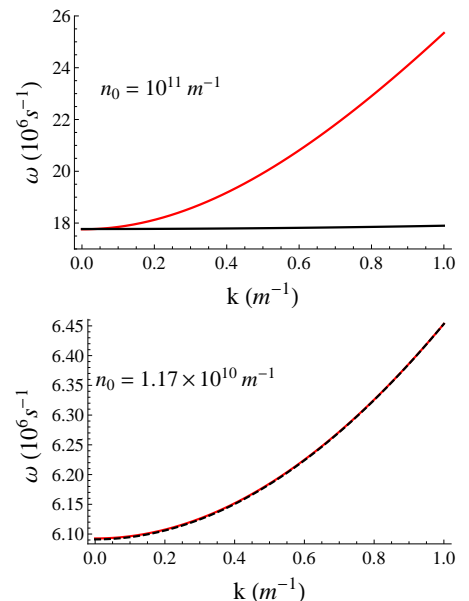

FIG. 11: A comparison between the relativistic and classical electron plasma (Langmuir-type) dispersion curve(s): the exact relation (8) in red and the classical non-relativistic in black (26). We have taken $T = 10^5 K$ in both cases. Note that the corresponding values of the relativistic parameter ξ_0 are $\xi_0 = 0.06$ in the upper panel and $\xi_0 = 0.007$ in the lower panel.

9. Therefore, the systems treated here are characterized by weak interactions (collisions), so that the relativistic Vlasov equation is applicable. As shown in Section IV,
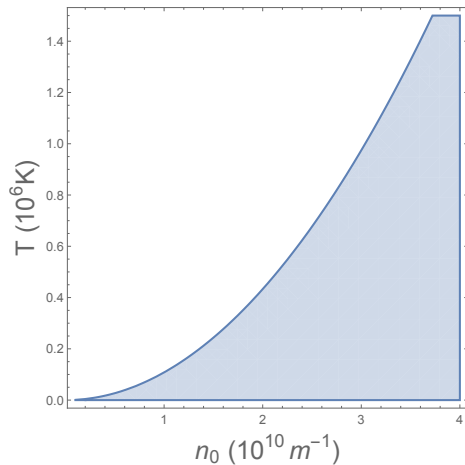
FIG. 12: The shaded region defines the range of density and temperature for which relativistic degenerate modeling is necessary (imposed); the interface denotes the curve $E_{Fe}/K_B T_e = 1$.

the fluid-theoretical results for linear waves are equiva-

lent to the obtained from kinetic-theoretical considerations (provided that the imaginary part of the dielectric function is negligible). In the high frequency limit, this amounts to a sufficiently large phase velocity to avoid wave-particle resonances, which is obeyed throughout.

[1] T. Giamarchi, *Quantum Physics in One Dimension* (Oxford University Press, New York, 2004).
[2] M. Passoni, L. Bertagna and A. Zani A., *New J. Phys.* **12**, 0450122 (2010).
[3] R. Thiele, P. Sperling, M. Chen *et al., Phys. Rev. E* **82**, 056404 (2010).
[4] P. K. Shukla and B. Eliasson, *Phys. Rev. Lett.* **100**, 036801 (2008).
[5] G. Barak, H. Steinberg, L. N. Pfeiffer *et al., Nature Physics* **6**, 489 (2010).
[6] A. Imambekov and L. I. Glazman, *Science* **323**, 228 (2009).
[7] F. Haas, G. Manfredi, P. K. Shukla and P.-A. Hervieux, *Phys. Rev. B* **80**, 073301 (2009).
[8] S. Ghosh, N. Chakrabarti and F. Haas, *Europhys. Lett.* **105**, 30006 (2014).
[9] V. N. Tsytovich, Sov. Phys. JETP **13**, 1249 (1961).
[10] B. Jancovici, Nuovo Ciemento **25**, 428 (1962).
[11] R. Hakim and J. Heyvaerts, Phys. Rev. A **18**, 1250 (1978).
[12] A. E. Delsante and N. E. Frankel, Ann. Phys. **125**, 137 (1980).
[13] F. Haas, *Quantum Plasmas: an Hydrodynamic Approach* (Springer, New York, 2010).
[14] Michael McKerr, Fernando Haas, Ioannis Kourakis, *Physical Review E*, **90**, 033112 (2014).
[15] F. Haas, J. Plasma Physics, **82** (6), 705820602 (2016).
[16] E. E. Salpeter, *Astrophys. J.* **134**, 669 (1961).
[17] M. McKerr, I. Kourakis and F. Haas, *Plasma Phys. Controll. Fusion* **56**, 035007 (2014).
[18] S. Chandrasekhar, *Mon. Not. R. Astron. Soc.* **95**, 207 (1935).
[19] P.-H. Chavanis, *Phys. Rev. D* **76**, 023004 (2007).
[20] A. Lenard, J. Math. Phys. **2**, 682 (1961).
[21] J. Dawson, Phys. Fluids **5**, 445 (1962).
[22] O. C. Eldridge and M. R. Feix, Phys. Fluids **6**, 398 (1963).
[23] J. L. Rouet and M. R. Feix, Phys. Plasmas **3**, 2538 (1996).
[24] L. Varela, G. Téllez and E. Trizac, Phys. Rev. E **95**, 022112 (2017).
[25] G. Téllez and E. Trizac, Phys. Rev. E **92**, 042134 (2015).
[26] S. Weinberg, Gravitation and Cosmology, (John Wiley and Sons, New York, 1972).
[27] F. Haas, J. Goedert, L. G. Garcia and G. Manfredi, *Phys. Plasmas* **10**, 3858 (2003).
[28] B. Eliasson and P. K. Shukla, *J. Plasma Phys.* **76**, 7 (2009).
[29] J. Bergman and B. Eliasson, *Phys. Plasmas* **8**, 1482 (2001).
[30] See e.g. in F.F. Chen, *Introduction to Plasma Physics and Controlled Fusion, Volume 1: Plasma Physics* (Plenum Press, N.Y. and London, 1974).
[31] M. McKerr, *Nonlinear Waves in Quantum Plasmas*, Doctoral Thesis, Queen's University Belfast (2016).
[32] Michael Mc Kerr, Fernando Haas, Ioannis Kourakis, *Physics of Plasmas*, **23**, 052120 (2016); DOI http://dx.doi.org/10.1063/1.4952774.
[33] V. Fortov, *Physics-Uspekhi* **6**, 615 (2006).